

Cell surface remodeling of *Mycobacterium abscessus* under cystic fibrosis airway growth conditions

Crystal J. Wiersma¹, Juan Manuel Belardinelli¹, Charlotte Avanzi¹, Shiva kumar Angala¹, Isobel Everall^{2,3}, Bhanupriya Angala¹, Edward Kendall¹, Vinicius Calado Nogueira de Moura^{1*}, Deepshikha Verma¹, Jeanne Benoit⁴, Karen P. Brown^{2,5}, Victoria Jones¹, Kenneth C. Malcolm^{6,7}, Michael Strong^{4,7}, Jerry A. Nick^{6,7}, R. Andres Floto^{2,5}, Julian Parkhill^{3,8}, Diane J. Ordway¹, Rebecca M. Davidson⁴, Michael R. McNeil¹, Mary Jackson^{1*}

From the ¹Mycobacteria Research Laboratories, Department of Microbiology, Immunology and Pathology, Colorado State University, Fort Collins, CO 80523-1682, USA; ²Molecular Immunity Unit, University of Cambridge Department of Medicine, MRC-Laboratory of Molecular Biology, Cambridge, CB2 0QH, UK; ³Wellcome Trust Sanger Institute, Hinxton, CB10 1SA, UK; ⁴Center for Genes, Environment and Health, National Jewish Health, Denver, CO 80206, USA; ⁵Cambridge Centre for Lung Infection, Papworth Hospital, Cambridge, CB2 0AY, UK; ⁶Department of Medicine, National Jewish Health, Denver, CO 80206, USA; ⁷Department of Medicine, University of Colorado, Anschutz Medical Campus, Aurora, CO 80045, USA; ⁸Department of Veterinary Medicine, University of Cambridge, Cambridge, CB3 0ES, UK

*Corresponding Author: Mary Jackson; Mary.Jackson@colostate.edu

Understanding the physiological processes underlying the ability of *Mycobacterium abscessus* to become a chronic pathogen of the cystic fibrosis (CF) lung is important to the development of prophylactic and therapeutic strategies to better control and treat pulmonary infections caused by these bacteria. Gene expression profiling of a diversity of *M. abscessus* complex isolates points to amino acids being significant sources of carbon and energy for *M. abscessus* in both CF sputum and synthetic CF medium, and to the bacterium undergoing an important metabolic reprogramming in order to adapt to this particular nutritional environment. Cell envelope analyses conducted on the same representative isolates further revealed unexpected structural alterations in major cell surface glycolipids known as the glycopeptidolipids (GPLs). Besides showing an increase in triglycosylated forms of these lipids, CF sputum- and synthetic CF medium-grown isolates presented as yet unknown forms of GPLs representing as much as 10 to 20% of the total GPL content of the cells, in which the classical amino alcohol located at the carboxy terminal of the peptide, alaninol, is replaced with the branched-chain amino alcohol, leucinol. Importantly, both these lipid changes were exacerbated by the presence of mucin in the culture medium. Collectively, our results reveal potential new drug targets against *M. abscessus* in the CF airway and point to mucin as an important host signal modulating the cell surface composition of this pathogen.

Keywords

Mycobacterium abscessus; cystic fibrosis; branched-chain amino acids; glycopeptidolipids; synthetic cystic fibrosis medium; mucin

The *Mycobacterium abscessus* complex (MABSC) is a group of opportunistic rapidly growing mycobacteria comprised of three subspecies, *Mycobacterium abscessus* subsp. *abscessus* (*Mabs*), *Mycobacterium abscessus* subsp. *massiliense* (*Mmas*), and *Mycobacterium abscessus* subsp. *bolletii*, that can cause an array of clinical diseases in human including lung, skin and soft tissue, central nervous system and disseminated infections. Recently, MABSC has become an important group of pathogens in the setting of CF lung disease¹⁻³. Of particular concern are the results of detailed epidemiology and population-level whole genome sequencing studies indicating that dominant circulating clones of MABSC have emerged and are now present on every continent⁴⁻⁶.

Understanding the complex physiological processes underlying the ability of MABSC to become a pathogen of the CF lung could provide valuable information on infection strategies of this organism and lead to innovative prophylactic and therapeutic strategies to better control and treat MABSC infections. One approach toward this goal has focused on analyzing the partial or whole genome sequence of serially-isolated strains from CF and non-CF patients to gain insight into the genetic basis of this adaptation⁶⁻⁸. These studies have highlighted a number of mutations, including those controlling the switching of MABSC from a smooth to rough morphotype, a process known to be related to the decrease or loss of production of surface glycopeptidolipids (GPLs) and to be associated with disease progression⁷⁻¹². The functional significance of other mutations is not as well understood and may benefit from the availability of a well-defined culture medium mimicking the nutritionally complex CF lung environment in which the stepwise adaptation of MABSC to various host-relevant stresses could be studied.

We here investigated how closely chemically defined synthetic CF medium (hereafter referred to as SCFM2)¹³ approximates the nutritional environment of actual CF sputum using a panel of genotypic and phenotypic read-outs. To this end, four *Mabs* and *Mmas* clustered (i.e., globally

circulating) and non-clustered isolates from CF patients were grown in SCFM2 and their gene expression profile and cell envelope composition were compared to those of the same strains grown in standard laboratory medium (7H9-ADC-Tween 80) or in actual CF sputum. Our results indicate that while MABSC grows at similar rates and to similar high cell densities in SCFM2 as in 7H9-ADC-Tween 80, it varies significantly in terms of gene expression profile and cell envelope composition, with SCFM2 being a much closer mimic of actual CF sputum. Collectively, our analyses point to amino acids being major sources of carbon and energy under CF-relevant growth conditions and to their utilization by the bacterium further causing important changes in the cell surface GPL composition of MABSC which are exacerbated by the presence of mucin in the culture medium.

Results

Growth characteristics of MABSC isolates in SCFM2 - Phenotypic and genotypic studies were conducted on both clustered (i.e., dominant, globally-circulating within the CF patient community) and non-clustered isolates of *M. abscessus* subsp. *abscessus* and *M. abscessus* subsp. *massiliense*, including strains with rough and smooth morphotypes. *Mabs* 1091 and *Mmas* 1239 are representative of dominant clades of *Mabs* and *Mmas* isolates whereas *Mmas* 184 and *Mmas* 604 are phylogenetically unrelated to any major clusters⁶. Further, *Mabs* 1091 is a rough morphotype isolate while all other strains are smooth. Although our study was not powered to typify potential clustered vs non-clustered, *Mabs* vs *Mmas*, or rough vs smooth specific responses to growth conditions, this strain selection ensured broad representation of the adaptive response of MABSC isolates to CF airway sputum.

As a first step toward characterizing the physiological response of MABSC to exposure to synthetic or actual CF sputum, we examined and compared the planktonic growth of the isolates in SCFM2, 7H9-ADC-Tween-80 and 20% CF sputum diluted in minimal M63 medium. All isolates grew to high cell density in SCFM2 with doubling times (~ 4.32 to 4.96 hours depending on the isolate) comparable to those observed in 7H9-ADC-Tween-80 (~ 4.70 to 4.94 hours) [Figure 1 and Figure S1].

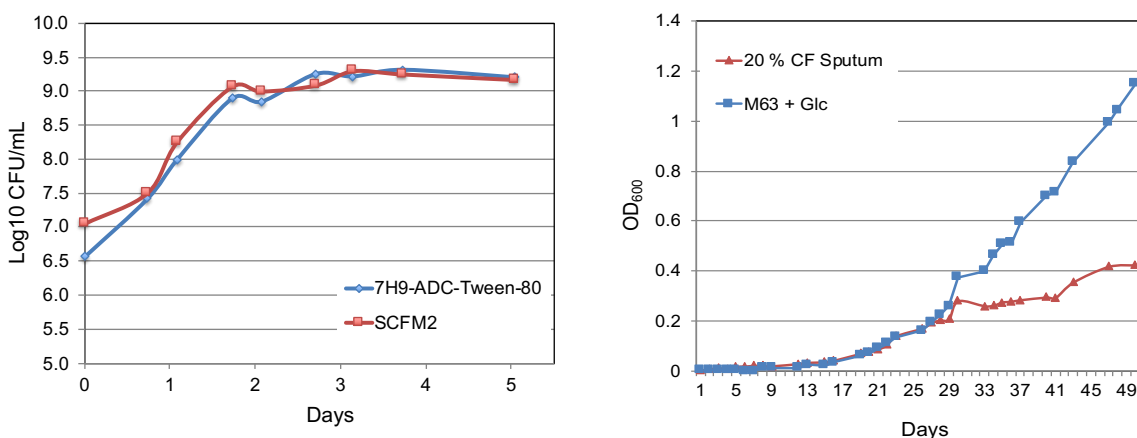


Figure 1: Growth characteristics of isolate *Mmas* 1239 at 37°C in 7H9-ADC-Tween-80, complete SCFM2 medium, CF sputum (diluted 20% in minimal M63 medium) and M63 medium supplemented with 0.2% glucose.

Growth in CF sputum, in contrast, was significantly slower and characterized by a long lag period followed by a period of slow replication (doubling time of ~ 18 days for *Mmas* 1239) [Figure 1]. Given that *Pseudomonas aeruginosa* grows as proficiently in 10% CF sputum and earlier generation synthetic CF medium¹⁴⁻¹⁵, this result is suggestive of the likely superior competitiveness of *P. aeruginosa* over MABSC during polymicrobial growth in CF sputum.

Increased production of triglycosylated and branched amino alcohol-containing forms of glycopeptidolipids by MABSC grown in SCFM2 and actual CF sputum - The unique cell envelope of mycobacteria is known to play important roles in the modulation of the innate and adaptive immune responses and in the resistance of mycobacterial pathogens to the bactericidal mechanisms of the host¹⁶. Surface GPLs in particular, which in the fast-growing nontuberculous *Mycobacterium*, *M. smegmatis*, have been shown to represent up to 85% of the surface-exposed lipids of the bacilli¹⁷, govern to a large extent the rough or smooth morphotype and planktonic vs biofilm growth of MABSC, and have been implicated in a number of virulence traits characterizing this microorganism^{9,11,18-27}. To determine whether the nutritional environment of CF airway sputum might affect the GPL composition of MABSC, the total lipids from *Mmas* isolates 1239, 184 and 604 grown to exponential phase in 7H9-ADC-Tween-80 and in complete SCFM2 were analyzed by liquid chromatography-mass spectrometry (LC-MS). Included in these analyses were the same three isolates grown in SCFM2 medium devoid of mucin, since host mucin glycans have been shown to regulate the cell surface properties and secretion of a number of virulence factors in the CF pathogen, *P. aeruginosa*²⁸. For comparison, *Mmas* isolate 1239 was also cultured in 10% CF sputum diluted in minimal M63 medium and in M63 containing 0.2% glucose as sole carbon source. The *Mabs* isolate 1091 which displays a rough morphotype and is essentially devoid of GPLs [Figure S2] was not included in this experiment.

LC-MS analysis of GPLs produced by the three *Mmas* isolates revealed the expected presence of diglycosylated and triglycosylated forms of these lipids in all strains. In general terms, MABSC diglycosylated GPLs consist of a tripeptide aminoalcohol (D-Phe- D-*allo*-Thr- D-Ala-L-alaninol) *N*-linked to a long (C₂₆ to C₃₄) 3-hydroxylated or 3-methoxylated fatty acyl chain, and substituted on the *allo*-Thr residue by a 3,4-*O*-diacetylated 6-deoxytalosyl unit, and on the terminal L-alaninol residue by a 3,4-di-*O*-methyl rhamnosyl unit²⁹ [Figure 2A]. In the triglycosylated forms, the 3,4-di-*O*-methyl-rhamnosyl unit is further glycosylated with a rhamnosyl unit at position 2 [Figure 2D]. Interestingly, a growth medium-dependent change in the relative proportion of tri- to diglycosylated GPLs was noted in all three isolates. This ratio increased 3.55-, 3.38- and 3.43-fold in *Mmas* 1239, 184 and 604 grown in complete SCFM2 relative to SCFM2 devoid of mucin, respectively [Figure 3A]. The ratios measured in 7H9-ADC-Tween-80 were intermediate between that measured in SCFM2 with and without mucin but much closer to the ratio measured in SCFM2 without mucin in two out of the three isolates. Importantly, a 1.86-fold increase in tri- relative to diglycosylated GPLs was also observed in *Mmas* 1239 grown in 10% CF sputum relative to M63-glucose [Figure 3A]. Collectively, these results are suggestive of the hyper-glycosylation of GPLs whenever mucin is present in the medium, either artificially in SCFM2 or in actual CF sputum.

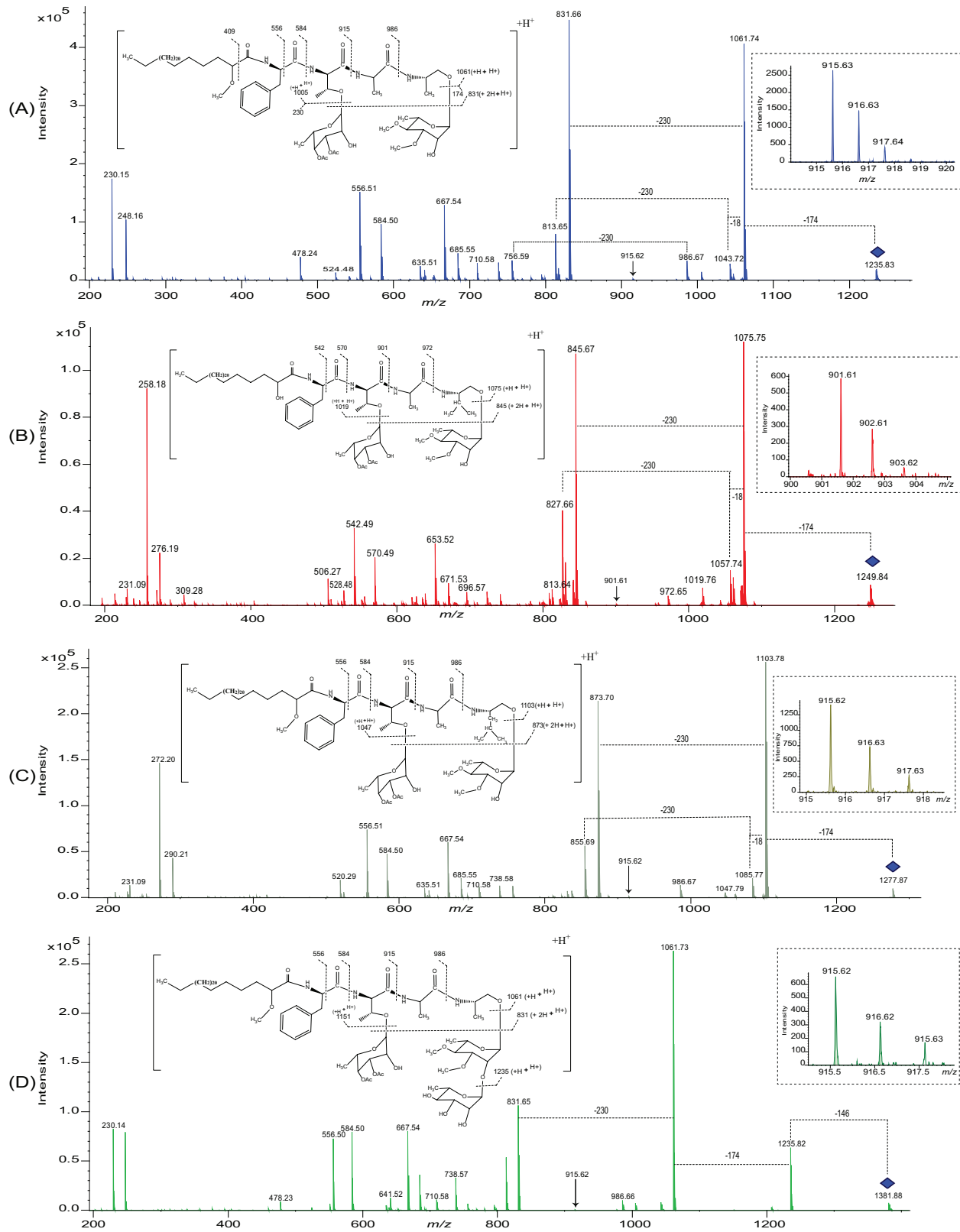


Figure 2: Structures of some of the major forms of GPLs produced by *Mmas* 1239, *Mmas* 184, and *Mmas* 604 in various media.

(A) MS/MS spectrum of the most abundant GPL with a molecular weight of 1234 Da containing a 2-methoxy C28 fatty acyl residue, a di-*O*-acetyl 6-deoxytalosyl residue (attached to the *allo*-threonine residue), and a 3,4 di-*O*-methyl rhamnosyl residue attached to the alaninol residue. The ion at m/z 556 shows the weight of the fatty acyl (2-methoxy C28 fatty acyl) substituent as attached to the phenylalanine. The ion at m/z 831 where both sugars have been eliminated shows the molecular weight of the entire acylated peptide and is consistent with the usual amino acids found in GPLs: phenylalanine, *allo*-threonine, and alanine) and the amino alcohol (alaninol) as shown in the figure. The sequence of the peptide is shown by the cleavages at the carbonyl carbons (B ions) at m/z 's 584, 915, and 986. The ion at m/z 1061 where the glycosyl residue attached to alaninol is lost shows the presence of two *O*-acetyl groups on the 6-deoxytalosyl residue. Also, this ion in combination with the M+H ion at m/z 1235 shows that the residue lost from the alaninol is the di-*O*-methyl rhamnosyl residue.

(B) The MS/MS spectrum of the GPL at m/z 1248 shows that the amino alcohol at the carboxy terminal of the peptide is 28 amu higher in molecular weight than alaninol. In this GPL, the ion at m/z 542 shows the presence of a 2-hydroxyl C28 fatty acyl component as it is 14 amu lower than the corresponding ion in panel (A), but the ion for the acylated peptide without the glycosyl components at m/z 845 is 14 amu higher than that in panel (A) showing that the peptide itself is 28 amu higher than expected. The B ions at m/z 's 570, 901 and 972 are consistent with the expected phenylalanine, *allo*-threonine and alanine showing that the extra 28 amu are on the amino alcohol unit. All the other ions in the spectrum (as discussed for panel A) are consistent with this assignment. Since our analysis of amino alcohols showed the presence of valinol (see Figure S2), we conclude that, in this GPL, valinol has been substituted for alaninol.

(C) MS/MS spectrum for the GPL with a molecular weight of 1276 Da which goes up in mucin-containing media (see Figure 3B). Analysis of the spectrum using the m/z values of the same cleavages discussed above for panels (A) and (B) shows that this GPL contains a 2-methoxy C28 fatty acyl group and that the amino alcohol is 42 amu heavier than alaninol. Since our analysis of amino alcohols showed the presence of leucinol (see Figure S2), we conclude that, in this GPL, leucinol has been substituted for alaninol.

(D) The MS/MS of a triglycosyl GPL with a molecular weight of 1380 Da which increased 1.6 to 2.1 fold in all three isolates grown in complete SCFM2 medium relative to SCFM2 without mucin (see Figure 3A) shows the presence of alaninol residue in the peptide, a 2-methoxy C28 fatty acyl group, and two *O*-acyl groups on the 6-deoxytalosyl residue. The ion at m/z 1225 in conjunction with the M+H ion at m/z 1381 shows that a non-methylated rhamnosyl residue is attached to a 3,4-di-*O*-methyl rhamnosyl residue which, as shown by the ion at m/z 1061, is attached to the alaninol residue.

Another intriguing observation that resulted from these analyses was the detection by LC-MS/MS of previously unreported forms of GPLs differing from the canonical forms described in Figure 2 A and D by the nature of their carboxy terminus aminoalcohol [Figure 2B-C]. Figure S3 presents gas chromatography-mass spectrometry (GC-MS) evidence for the branched-chain amino alcohols, valinol or leucinol, indeed replacing the prototypical alaninol in predominant forms of these atypical GPL species identified in all isolates. While these atypical forms of GPLs were found in all isolates independent of the culture medium, the production of one of them - a diglycosylated leucinol-containing form with m/z 1276 [Figure 2C] - increased sharply (1.8 to 3.4-fold) in all three strains grown in complete SCFM2 relative to SCFM2 without mucin, representing as much as 8.8 to 23.6% of total GPLs in the SCFM2-grown cells and 9.5% of total GPLs in CF sputum-grown *Mmas* 1239 [Figure 3B]. The abundance of this GPL species was 5.8 to 8.4-fold greater in strains grown in complete SCFM2 relative to 7H9-ADC-Tween-80 and also increased 1.5-fold in *Mmas* 1239 grown in 10% CF sputum relative to M63-glucose [Figure 3B]. Changes in other GPL forms were either not consistent across isolates, or not SCFM2-dependent, or not recapitulated in 10% CF sputum. Collectively, these findings indicate that MABSC undergoes significant cell surface remodeling under CF-relevant growth conditions and that mucin plays a central regulatory role in the process.

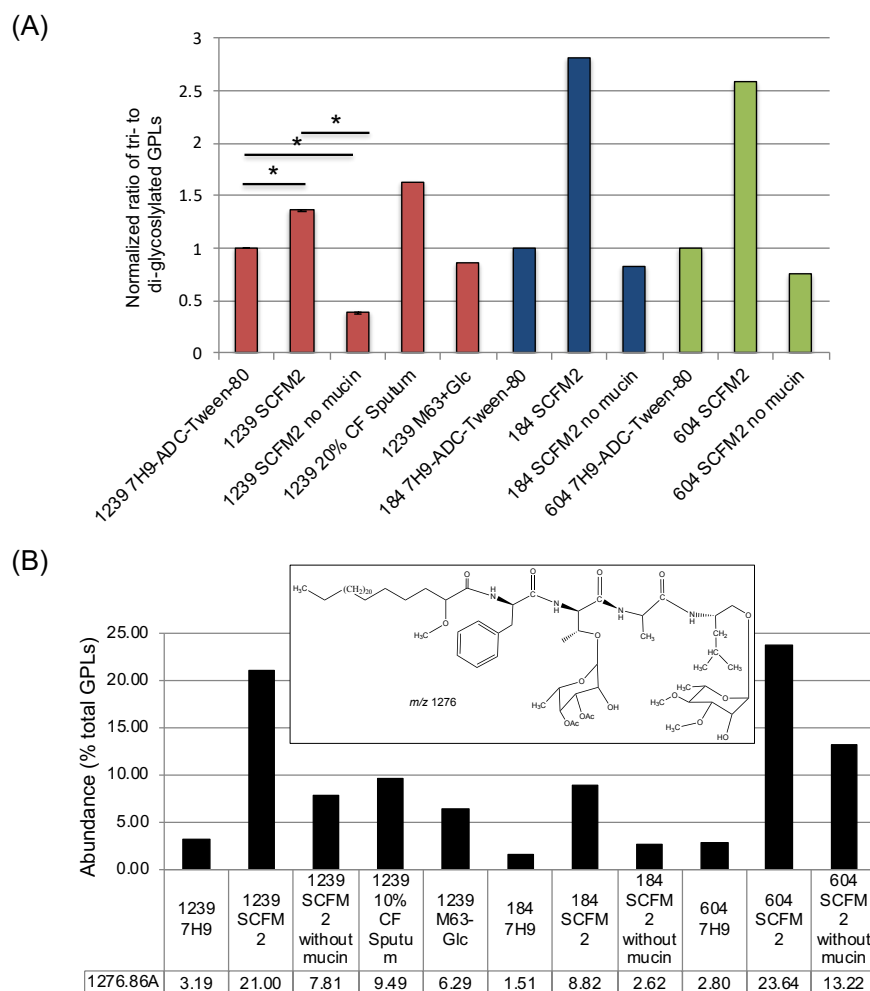


Figure 3: Changes in the GPL content of MABSC isolates grown in SCFM2 complete medium and in CF sputum. (A) Mucin-dependent increase in the ratio of tri- to di-glycosylated GPLs. Di- to tri-glycosylated GPL ratios in *Mabs* 1239, *Mmas* 184 and *Mmas* 604 grown in SCFM2, SCFM2 without mucin, 7H9-ADC-Tween-80, 10% CF sputum or M63-glucose are expressed relative to the ratio measured in the strains grown in 7H9-ADC-Tween-80 arbitrarily set to 1. Two independent batches of 7H9-ADC-Tween-80 and SCFM2 (with and without mucin)-grown *Mmas* 1239 were analyzed and averages and standard deviations are shown. Asterisks denote statistical significance per Student's *t*-test ($p < 0.05$).

(B) Build-up of a leucinol-containing form of diglycosylated GPL in MABSC isolates grown in SCFM2 complete medium and in 10% CF sputum. Evidence for the accumulation of a diglycosylated form of GPL with *m/z* 1276 in *Mabs* 1239, *Mmas* 184 and *Mmas* 604 grown in complete SCFM2 and 10% CF sputum relative to 7H9-ADC-Tween-80 and SCFM2 lacking mucin. The percentage abundance of this GPL form in each isolate and each medium relative to total GPLs is indicated beneath the graph. The “total” GPL content of the cells was calculated using the 26 most abundant forms of these lipids which collectively were estimated to represent > 85% of the GPL content of all isolates.

Other cell envelope analyses conducted on the isolates grown in the different media, including total (glyco)lipid content [Figure S4A and LC-MS data not shown], monosaccharide content of extractable lipids and delipidated cells [Table S1], and mycolic acid composition [Figure S4B] failed to reveal any significant qualitative or quantitative differences between strains or growth conditions.

Transcriptional profiling of MABSC grown in 7H9-ADC-Tween-80 versus actual and synthetic CF airway sputum reveals extensive metabolic reprogramming related to amino acid utilization

- Transcriptional profiling of the four MABSC clinical isolates grown to exponential phase in 7H9-ADC-Tween 80, SCFM2 complete medium or 20% CF sputum was next performed using RNA-sequencing to investigate the most significant changes in physiology between MABSC grown in classical 7H9-ADC-Tween 80 laboratory medium and SCFM2, and to determine how closely SCFM2 mimics the physiological state of MABSC in actual patient sputum. For each isolate, genes were identified that showed ≥ 2 Log₂ fold-change in expression between culture conditions with a false discovery rate adjusted *p*-value ≤ 0.05 . Isolates were further compared between them for common differentially regulated genes. Owing to the limited quantities of patient sputum available for these studies, gene expression profiling in 20% sputum was only performed on the clustered *Mmas* isolate 1239.

The number and lists of genes differentially expressed in the different culture conditions for each isolate are presented in Figure 4A and Tables S2A-E. In all isolates, there were more genes expressed at a higher level in SCFM2 compared to 7H9-ADC-Tween 80 than there were genes expressed at a lower level. Twenty-six genes were expressed at higher level in all four isolates in SCFM2 relative to 7H9-ADC-Tween 80 [Tables S2A-D]. Given the strong overlap in gene expression profiles between isolates, a strain independent response to media was calculated by pooling all SCFM2 samples and all 7H9-ADC-Tween 80 samples from all four isolates for differential expression analysis. In this analysis, 60 genes had significantly higher expression in SCFM2 than 7H9-ADC-Tween 80 and 21 genes were expressed at significantly lower level in SCFM2 [Table 1].

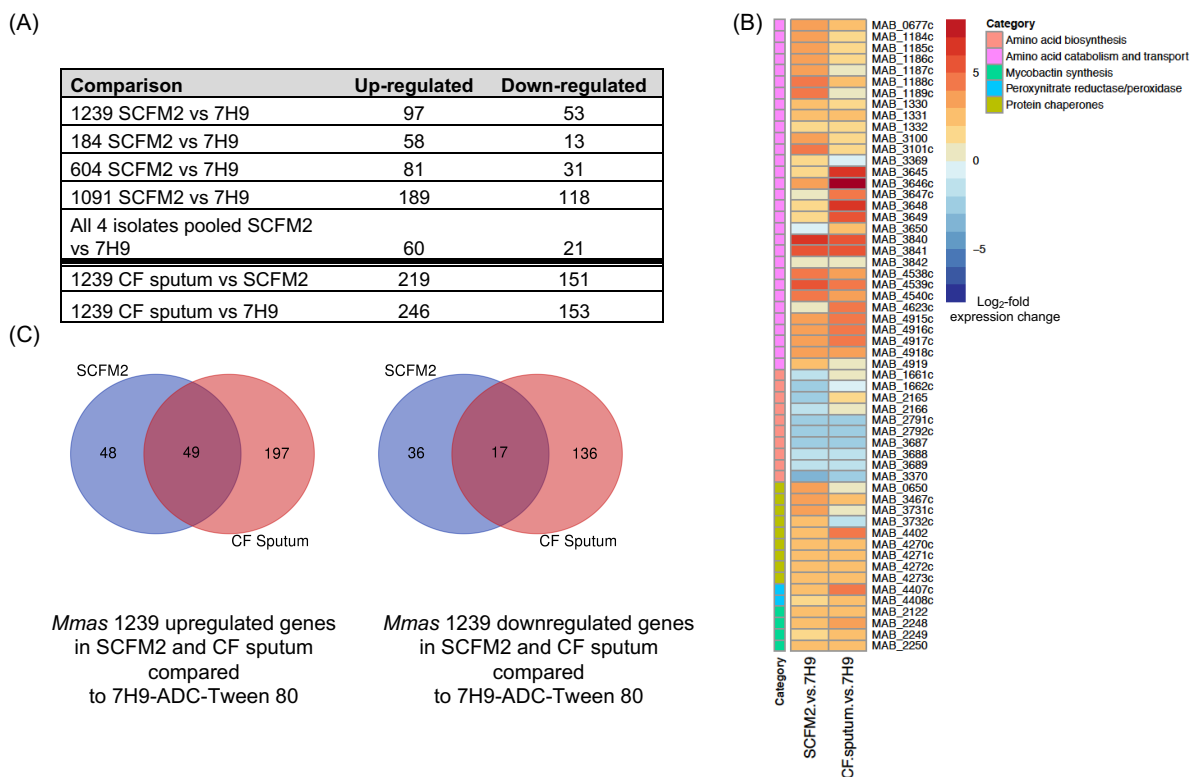


Figure 4: Transcriptional response of MABSC to SCFM2 and actual CF sputum.

(A) Number of genes in each isolate expressed at higher or lower level in SCFM2 when compared to 7H9-

ADC-Tween 80, or in CF sputum when compared to 7H9-ADC-Tween 80 or SCFM2. Most divergent from other isolates was *Mabs* 1091 which displayed the highest number of both up- and down-regulated genes in SCFM2 compared 7H9-ADC-Tween 80 [see Table S2D]. It is unclear at this point whether the differentially expressed genes unique to this isolate are the result of its rough morphotype or related to the different MABSC subspecies or clone to which it belongs.

(B) Heatmap showing the Log₂ fold-change of *Mmas* 1239 transcripts in SCFM2 and CF sputum relative to 7H9-ADC-Tween 80.

(C) Venn diagrams showing number of genes expressed at significantly higher or lower level in *Mmas* 1239 in CF sputum and SCFM2 compared to 7H9-ADC-Tween 80. The complete list of these genes is provided in Table S2F.

Table 1: List of genes that were expressed at higher or lower levels in SCFM2 than in 7H9-ADC-Tween 80, independent of MABSC isolate. More or less highly expressed genes in SCFM2 were defined as ≥ 2 Log₂ fold-change in expression compared to cells grown in 7H9-ADC-Tween 80, with a false discovery rate adjusted *p*-value (padj) <0.05. Base mean is the mean of the gene counts in SCFM2- and 7H9-ADC-Tween 80-grown bacteria. Genes in bold were found to be similarly differentially regulated in CF sputum relative to 7H9-ADC-Tween 80 (see Table S2F). Similarly colored genes denote gene clusters.

Proposed Function	Gene_id	Gene Name	Gene Product	base mean	log ₂ fold change	padj
Pooled SCFM2 vs 7H9-ADC-Tween 80 upregulated genes						
MSF transporter	MAB_0069		Major facilitator family transporter	620	2.6	6.97E-09
-	MAB_0304		Hypothetical protein	86	3.2	0.001599021
Protein chaperone	MAB_0650	groEL2	60 kDa chaperonin 2 (Protein Cpn60 2)	109891	2.5	5.96E-27
-	MAB_1030		Hypothetical protein	3617	2.0	0.000297421
Amino acid metabolism (Val catabolism)	MAB_1184c		Putative transcriptional regulator, MarR family	816	2.5	5.68E-19
	MAB_1185c		Probable enoyl-CoA hydratase	3400	2.4	2.04E-23
	MAB_1186c	mmsB	3-hydroxyisobutyrate dehydrogenase	2234	2.4	1.20E-29
	MAB_1187c		Probable enoyl-CoA hydratase	3550	2.5	8.73E-31
	MAB_1188c		Probable acyl-CoA dehydrogenase	2952	3.7	4.55E-27
MAB_1189c	mmsA	Probable methylmalonic acid semialdehyde dehydrogenase	4478	3.2	3.92E-40	
Amino acid metabolism (Arg and Pro catabolism)	MAB_1330	rocA	1-pyrroline-5-carboxylate dehydrogenase	32153	3.8	1.27E-111
	MAB_1331		Probable proline dehydrogenase	10679	3.8	1.72E-172
	MAB_1332	fadD	Probable fatty-acid-CoA ligase FadD	2905	2.1	1.83E-44
Mycobactin synthesis	MAB_2122	mbtE	Putative peptide synthetase	462	2.1	1.93E-12
	MAB_2248	mbtE	Probable peptide synthetase	236	2.0	3.88E-08
	MAB_2249	mbtG	Probable lysine-N-oxygenase	168	2.0	2.99E-09
MSF transporter	MAB_2273		Putative MFS transporter	1024	2.4	1.00E-80
Amino acid metabolism (Ala catabolism)	MAB_3100	ald	L-alanine dehydrogenase	45451	5.4	1.10E-40
	MAB_3101c		Hypothetical protein – putative reductase	11584	5.1	5.50E-118
-	MAB_3153c		Hypothetical protein	68	2.8	7.23E-15
	MAB_3154c		Hypothetical protein	165	2.8	1.64E-24
-	MAB_3180		Hypothetical membrane protein	103	3.1	1.87E-74
Amino acid transport	MAB_3369		Putative integral membrane amino acid transport protein	402	3.0	1.52E-22
-	MAB_3385		Hypothetical protein – putative transcriptional regulator	788	3.7	3.56E-13
	MAB_3386c		Hypothetical membrane protein	1388	4.2	1.30E-20
-	MAB_3438		Putative short-chain dehydrogenase/reductase	129	2.7	0.035324512
Protein chaperone	MAB_3467c		18 kDa antigen (HSP 16.7)	6073	3.0	3.11E-18
-	MAB_3617		Hypothetical protein	411	2.3	1.64E-23
Amino acid metabolism (Lys catabolism)	MAB_3645		Putative reductase	2202	5.4	2.88E-30
	MAB_3646c	lat	L-lysine aminotransferase	32693	7.9	6.83E-41
	MAB_3647c	lprA	Probable AsnC transcriptional regulatory protein	3836	3.5	4.24E-22
	MAB_3648		Hypothetical protein	6468	5.9	2.53E-31
	MAB_3649	pcd	Probable piperideine-6-carboxylate dehydrogenase	22782	5.8	4.43E-33
MAB_3650		Putative TetR-family transcriptional regulator	2276	3.2	2.30E-16	
Protein chaperones	MAB_3731c	groEL1	60 kDa chaperonin 1	6834	2.0	2.91E-12
	MAB_3732c	groES	10 kDa chaperonin	59928	2.1	7.43E-15
-	MAB_3762		Hypothetical protein	959	3.1	2.84E-23
Amino acid metabolism (Arg catabolism)	MAB_3840		Amidinotransferase family protein	6816	7.2	5.72E-157
	MAB_3841	rocD1	Ornithine aminotransferase	4795	5.9	1.15E-76
	MAB_3842	rocE	Probable arginine permease (integral membrane protein)	3592	2.1	1.12E-17

Proposed Function	Gene_id	Gene Name	Gene Product	base mean	log ₂ fold change	padj
Protein chaperone	MAB_4402		Heat shock protein Hsp20	288	2.3	1.08E-05
Pooled SCFM2 vs 7H9-ADC-Tween 80 upregulated genes (continued)						
Peroxynitrite reductase/ peroxidase	MAB_4407c	ahpD	Putative alkylhydroperoxidase	880	3.0	2.34E-28
	MAB_4408c	ahpC	Putative alkylhydroperoxidase C	1550	2.4	5.76E-30
Amino acid metabolism (Leu catabolism)	MAB_4538c	fadE	Putative acyl-CoA dehydrogenase	2341	4.2	1.81E-136
	MAB_4539c	accA	Putative acyl-CoA carboxylase alpha subunit	2315	4.5	4.45E-137
	MAB_4540c	accD	Putative methylcrotonoyl-CoA-carboxylase	1981	4.6	7.90E-138
Amino acid metabolism (Met)	MAB_4623c		5-methyltetrahydropteroyltriglutamate--homocysteine S-methyltransferase	2569	2.4	1.44E-07
-	MAB_4735		Putative starvation-induced DNA protecting protein/Ferritin and Dps	163	2.2	0.000500508
-	MAB_4742c		Putative methyltransferase	14035	5.1	5.60E-80
	MAB_4743c		Putative dehydrogenase/reductase	33256	7.6	4.70E-198
	MAB_4744c		DsbA-like thioredoxin domain protein	14307	8.0	7.85E-187
	MAB_4745	mmpS	Putative membrane protein	2277	7.8	1.07E-143
	MAB_4746	mmpL	Putative membrane protein	15104	8.1	9.78E-97
	MAB_4747		Putative copper-sensing transcriptional repressor	5091	4.4	1.19E-82
	MAB_4748c		Putative pyridoxamine 5'-phosphate oxidase	1406	4.0	4.14E-53
Amino acid metabolism (catabolism of branched amino acids, Val, Leu, Ile)	MAB_4915c		Hypothetical protein – PknH-like extracellular domain protein	458	3.5	1.55E-134
	MAB_4916c	bkdC	Probable branched-chain keto acid dehydrogenase E2 component	8541	4.4	6.15E-116
	MAB_4917c	bkdB	Probable branched-chain keto acid dehydrogenase E1 component, beta subunit	4900	4.0	6.13E-19
	MAB_4918c	bkdA	Probable branched-chain keto acid dehydrogenase E1 component, alpha subunit	6217	3.8	1.20E-12
	MAB_4919		Putative transcriptional regulator, AsnC family	237	2.2	9.98E-18
Proposed function	Gene_id	Gene Name	Gene Product	base mean	log ₂ fold change	padj
Pooled SCFM2 vs 7H9-ADC-Tween 80 downregulated genes						
-	MAB_0741c		Hypothetical protein	750	-2.4	4.62E-18
Manganese transport	MAB_1031c	mntH	Probable manganese transport protein MntH	2211	-3.4	1.22E-26
Amino acid metabolism (Cys biosynthesis)	MAB_1661c	cysH	Phosphoadenosine phosphosulfate reductase (CysH)	940	-2.1	2.24E-17
	MAB_1662c		Probable sulfite reductase [ferredoxin]	2127	-2.4	8.11E-58
Cytochrome P450	MAB_2048c		Probable cytochrome P450	8405	-2.5	0.033135945
Amino acid metabolism (Val and Ile biosynthesis)	MAB_2165		Probable acetolactate synthase, large subunit	145	-2.4	8.93E-11
	MAB_2166		Hypothetical protein	294	-2.1	2.41E-08
-	MAB_2551		Hypothetical protein	204	-2.2	2.80E-17
-	MAB_2599		Hypothetical protein	153	-2.2	8.07E-26
	MAB_2600		Hypothetical protein	160	-2.0	6.02E-34
	MAB_2601		Hypothetical protein	250	-2.4	2.90E-22
-	MAB_2693		Hypothetical protein	322	-6.0	3.90E-24
Amino acid metabolism and transport?	MAB_2791c		Putative ethanolamine permease	581	-2.2	8.67E-06
	MAB_2792c		Probable aldehyde dehydrogenase	1088	-2.7	8.97E-08
-	MAB_3359c		GCN5-related N-acetyltransferase	454	-2.2	0.000366436
Amino acid metabolism (Met biosynthesis)	MAB_3687	metC	Probable O-acetylhomoserine sulfhydrylase MetC (homocysteine synthase)	1664	-2.2	4.33E-21
	MAB_3688	metA	Homoserine O-acetyltransferase	1230	-2.2	3.71E-108
	MAB_3689		Putative methyltransferase	362	-2.2	2.18E-111
-	MAB_3903		Hypothetical protein (nitroreductase?)	7602	-2.2	0.041104308
Cytochrome P450	MAB_4456		Putative cytochrome P450	708	-2.1	3.46E-12
-	MAB_4715c		Conserved hypothetical protein	2782	-4.4	1.17E-11

Pathway enrichment analysis using Kyoto Encyclopedia of Genes and Genomes (KEGG) and manually curated pathways indicated that cellular processes that were significantly induced in SCFM2 relative to 7H9-ADC-Tween 80 were disproportionately dominated by pathways for amino acid catabolism (branched-chain amino acids [leucine, valine and isoleucine], arginine, lysine, proline, alanine) and central carbon metabolism as it relates to pyruvate, lactate, glutamate, acetoacetic acid, propionyl-CoA and acetyl-CoA. Downregulated genes in SCFM2 were mostly for amino acid biosynthesis [Figure 4B; Table 1; Tables S2A-D]. Despite noticeable changes in the GPL composition of the isolates grown in SCFM2 relative to 7H9-ADC-Tween 80 [Fig. 3], the transcript levels of GPL biosynthetic genes²⁹ were not statistically different between the media for any of the isolates.

Comparison of differentially expressed genes in *Mmas* 1239 grown in 20% CF sputum vs 7H9-ADC-Tween 80 and SCFM2 vs 7H9-ADC-Tween 80 identified 49 genes expressed at a significantly higher level in both SCFM2 and 20% CF sputum and 17 genes expressed at a significantly lower level in both media [Figure 4C and Table S2F]. Many of these genes are identical to those listed in Table 1 or fall in the same functional categories (see Figure 4B and genes highlighted in bold letters in Table 1).

Mmas 1239 genes differentially expressed in CF sputum but not in SCFM2 relative to 7H9-ADC-Tween 80 or, vice versa, differentially expressed in SCFM2 but not in CF sputum relative to 7H9-ADC-Tween 80 (based on a ≥ 2 Log₂ fold-change cut-off) are listed in Table S2G. For the most part, these genes followed the same trend in both media despite showing differences in their level of expression.

Real-time PCR confirmed the *Mmas* 1239 RNAseq data for five differentially expressed genes of interest: *MAB_2157* (a putative fatty acid desaturase), *ahpD* (*MAB_4407c*), *bkdC* (*MAB_4916c*), *MAB_4742c* and *MAB_4743c* [Figure S5].

Growth characteristics of BCKADH and GPL-deficient Mmas knock-out mutants in SCFM2 -

Transcriptional profiling and lipid analyses converging to indicate that branched-chain amino acids (BCAAs) are major drivers of the physiological reprogramming undergone by MABSC under conditions relevant to the CF airway, we next sought to determine the effect of disrupting genetically the production of GPLs (including leucinol-containing forms of these lipids) or the branched-chain keto acid dehydrogenase (BCKADH) enzyme on the growth of MABSC in culture media containing various concentrations of BCAAs. Deletion mutants in the *bkdA-bkdB-bkdC* and *mmpL4b* genes (the latter gene being required for GPL biosynthesis)²⁹ were generated by recombineering in the reference strain *Mmas* CIP108297 [Figure S6A]. In complete SCFM2 medium, which contains other carbon sources besides BCAAs (including lactate, glucose, mucin and, in this case, 0.25% Tween 80 to facilitate CFU counting), the two mutants replicated comparably to the wild-type (WT) strain, despite the GPL-deficient strain consistently reaching a slightly lower cell density [Figure S6B].

To more precisely determine the response of the BCKADH knock-out to BCAA levels, we next compared the growth of this mutant to that of its WT parent in minimal medium containing different concentrations of the individual or mixed BCAAs. Whereas the growth of the WT strain generally increased with increasing concentrations of BCAAs in the medium (both in terms of growth rate and maximum cell density), the BCKADH mutant displayed dramatically (~ 10-fold) reduced growth at 1x BCAA and was on the contrary inhibited by high concentrations of BCAAs reflective of its limited ability to process this carbon source and of the toxic build-up of branched-chain keto acids in the cells when BCAAs are the sole carbon source in the culture medium [Figure

5A]. In line with this observation, the mutant also grew very poorly when leucine, isoleucine or valine were used as sole carbon sources whereas it grew similarly to the WT parent strain in the presence of glucose [Figure 5B]. Of the three BCAAs, leucine was the preferred carbon source for WT *Mmas* CIP108297 followed by isoleucine. Valine was the least effective at supporting growth [Figure 5B].

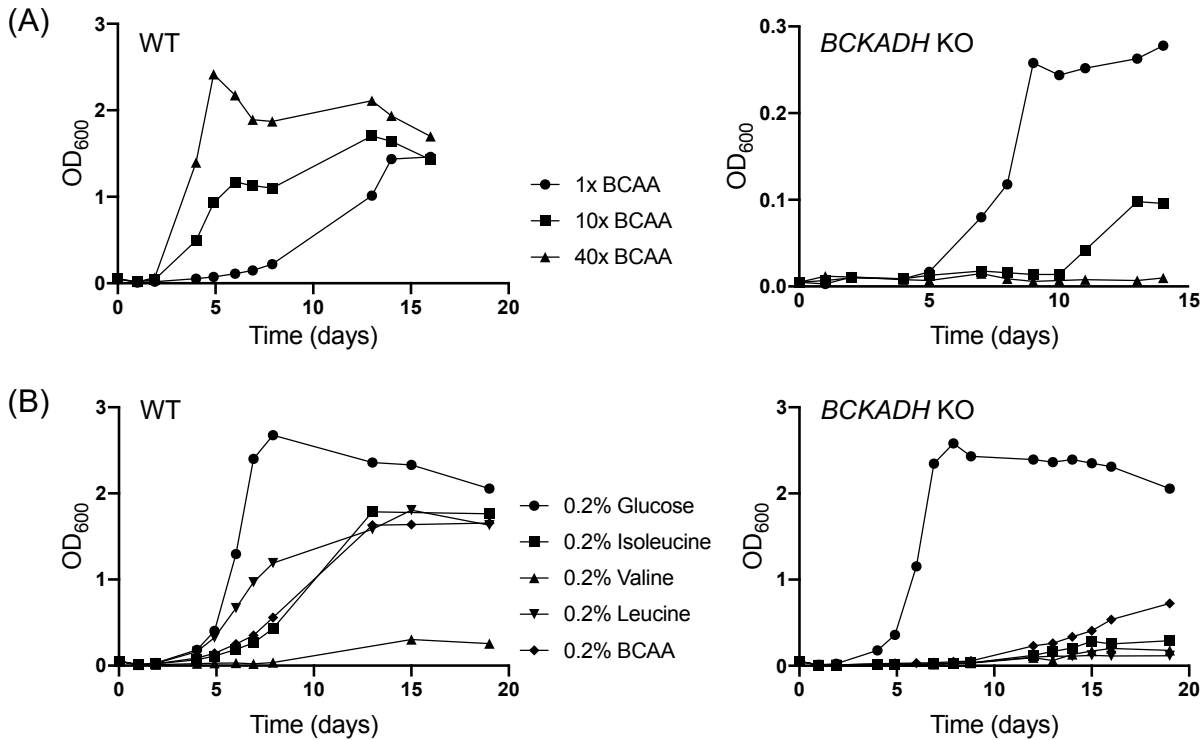


Figure 5: Growth characteristics of the BCKADH mutant in branched amino acid-containing media. The results presented are representative of two independent experiments using different culture batches (biological replicates).

(A) Growth of WT *Mmas* CIP108297 and the BCKADH-deficient mutant in minimal medium containing either the concentration of BCAAs normally found in SCFM2 (1x) or 10- or 40-times this amount. Note the 10-fold difference in Y-axis scale between the WT and mutant strains.

(B) Growth of WT *Mmas* CIP108297 and the BCKADH-deficient mutant in minimal medium containing 0.2% glucose, 0.2% equimolar BCAA mix, or 0.2% of each of the individual BCAAs, valine, leucine and isoleucine.

In line with our observations made on clinical isolates from patients with CF, the production of the dominant leucinol-containing form of GPL [Figure 2C and 3B] was increased both in the WT and BCKADH mutant grown in complete SCFM2 medium relative to 7H9-ADC-Tween 80. This increase, however, was significantly more marked in the mutant strain (2.47-fold \pm 0.14 in the mutant vs 1.46-fold \pm 0.11 in the WT parent; averages and SD of biological triplicates).

Virulence attenuation of MABSC grown in SCFM2 - Since changes in the cell surface composition and overall metabolism of MABSC caused by the different growth conditions may have impacted the way the bacterium interacted with host cells, we next compared the uptake and intracellular replication of *Mmas* 1239 and *Mmas* 184 grown either in 7H9-ADC-Tween-80,

SCFM2 or SCFM2 without mucin, in THP-1 monocyte-derived macrophages and A549 epithelial cells. Overall, while no significant difference in cellular uptake was noticeable between growth conditions, the isolates grown in SCFM2 (with or without mucin) showed decreased intracellular replication compared to 7H9-ADC-Tween-80-grown bacilli, especially in THP-1 cells [Figure 6]. SCFM2-grown MABSC thus appears to be less prepared for intracellular survival, a finding that may be explained by the fact that MABSC bacilli growing in airway sputum, whether planktonically or within biofilms, are expected to be mainly extracellular.

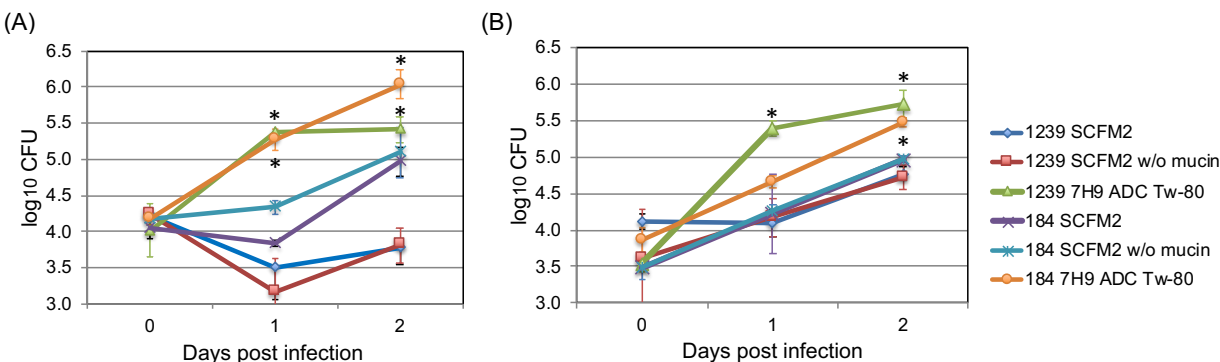


Figure 6: Uptake and intracellular replication of *Mmas* 1239 and *Mmas* 184 in human THP-1 monocyte-derived macrophages (A) and A549 epithelial cells (B).

Isolates were grown either in 7H9-ADC-Tween-80, SCFM2 complete medium or SCFM2 without mucin and used to infect the cells at a multiplicity of infection of 10. Data is shown as mean values + SD of triplicate wells. *Mmas* 1239 grown in 7H9-ADC-Tween-80 replicates significantly more after one or two days than the same isolate grown in SCFM2 with or without mucin in both cell types [asterisks denote statistical significance per Student's *t*-test ($p < 0.05$)]. *Mmas* 184 grown in 7H9-ADC-Tween-80 replicates significantly more than the same isolate grown in SCFM2 with or without mucin in THP-1 cells after one or two days, and in A549 cells after 2 days. The results presented are representative of two independent experiments.

Comparative antibiotic susceptibility profile of MABSC clinical isolates grown in SCFM2 versus cation-adjusted Mueller Hinton II - A current obstacle to the informed treatment of MABSC infections is the lack of correlation between *in vivo* and *in vitro* antibiotic susceptibility for most antibiotics with the exception of macrolides³. This limitation finally prompted us to determine if the susceptibility of isolates grown in SCFM2, which our results indicate are physiologically closely related to bacteria grown in CF sputum, was the same as the susceptibility measured in cation-adjusted Mueller-Hinton II broth. We tested a panel of fifteen clinically-relevant antibiotics against fifteen (drug-susceptible and drug-resistant) MABSC reference strains and clinical isolates [Tables 2 and S3]. Furthermore, Minimum Inhibitory Concentrations (MICs) for three strains were tested both in complete SCFM2 medium and in SCFM2 devoid of mucin to determine the impact of mucin on MICs [Table 2]. Overall, MIC values measured in Mueller-Hinton II broth and SCFM2 without mucin were very consistent, differing by two-fold or less which is deemed within the margin of experimental error and culture-to-culture variability. There were also very few instances of greater than 4-fold increases in MIC values in complete SCFM2 relative to SCFM2 without mucin [Table 2]. As this was not an antibiotic-specific trend but rather isolated, strain-dependent, instances of varied susceptibility, we conclude that drug susceptibility determination in SCFM2 (with or without mucin) as described herein is unlikely to be more predictive of clinical outcome than the Clinical and Laboratory Standards Institute protocol.

Table 2: MIC values against *Mabs* and *Mmas* reference strains and clinical isolates in cation-adjusted Mueller Hinton II broth, complete SCFM2 and SCFM2 devoid of mucin.

MIC values are in µg/mL. Greater than 4-fold changes in MIC values between complete SCFM2 medium and SCFM2 without mucin or cation-adjusted Mueller Hinton II broth are highlighted in green. nd, not determined. MIC determinations were performed on two to three independent culture batches. MICs in complete SCFM2 medium for each isolate essentially focused on antibiotics with MICs < 64 µg/mL and were completed on one culture batch.

Antibiotic	<i>Mabs</i> ATCC 19977			<i>Mmas</i> CIP 108297			<i>Mmas</i> 1239			<i>Mmas</i> 604		<i>Mabs</i> 1091		<i>Mmas</i> 184	
	MH-II	SCFM2	SCFM2 w/o mucin	MH-II	SCFM2	SCFM2 w/o mucin	MH-II	SCFM2	SCFM2 w/o mucin	MH-II	SCFM2 w/o mucin	MH-II	SCFM2 w/o mucin	MH-II	SCFM2 w/o mucin
Amikacin	16	64	8	64	nd	64	32	64	64	128	64	32	16	256	>256
Apramycin	32	nd	32	4	8	4	2	8	1	2	1	4	2	2	1
Azithromycin	>160	nd	>160	1.25	10	2.5	>160	nd	>160	1.25	2.5	>160	>160	2.5	2.5
Clarithromycin	160	nd	160	0.08	0.64	0.16	>160	nd	>160	0.16	0.32	80	40	0.16	0.32
Erythromycin	>256	nd	>256	8	40	8	>256	nd	>256	2	8	>256	>256	8	4
Kanamycin	8-16	32	8	8	16	8	16	16	8	32	64	32	32	16	32
Ethambutol	160	nd	80	160	nd	160	320	nd	320	320	320	160	320	160	320
Rifampicin	>320	nd	>320	>320	nd	>320	>320	nd	>320	>320	>320	>320	>320	>320	>320
Streptomycin	128	128	64	8	8	4	32	128	64	256	128	128	128	>256	>256
Cefoxitin	100	50	50	50	50	50	50	50	100	25	100	100	100	25	50
Tobramycin	64	128	32	16	128	16	128	nd	64	>256	>256	64	64	>256	256
Linezolid	32	128	64	8	128	16	4	32	4	8	16	8	16	8	16
Tetracycline	>160	nd	>160	20	40	20	nd	nd	nd	>160	>160	>160	>160	>160	>160
Imipenem	64	nd	64	128	64	64	64	nd	128	nd	nd	256	>256	32	64
Ciprofloxacin	32	16	64	64	64	64	64	32	128	64	64	64	64	32	64

Discussion

The results presented herein indicate that, despite not fully recapitulating all of the nutritional complexity and variety of stresses present in CF sputum, SCFM2 is clearly a closer proxy of actual CF sputum than 7H9-ADC-Tween 80 both in terms of transcriptional profile and surface lipid composition. Gene expression profiling and cell envelope analyses of four clustered and non-clustered *Mmas* and *Mabs* isolates unambiguously pointed to amino acids, particularly lysine, alanine, proline, arginine and BCAAs being significant sources of carbon and energy for MABSC in both CF sputum and SCFM2, and to MABSC undergoing important cell surface and metabolic reprogramming in order to adapt to this particular nutritional environment. In this respect, our RNA-seq results confirm previous observations made by Miranda Caso-Luengo and collaborators on the initial transcriptional response of *Mabs* ATCC 19977 precultured in 7H9-ADC-Tween-80 to a short-pulse (3-hour) exposure to SCFM2³⁰ (despite the mis-annotation in this earlier study of the *BCKADH* gene cluster as encoding a pyruvate dehydrogenase complex). *bkdA*, *bkdB* and *bkdC*, and other genes related to the catabolism of BCAAs, were among the most induced in SCFM2 and CF sputum relative to 7H9-ADC-Tween 80 [Table 1]. The requirement of BCKADH for optimal growth in BCAA-containing medium was further obvious from the dramatically reduced replication of a *bkdA-bkdB-bkdC* *Mmas* deletion mutant compared to its WT parent in minimal medium containing BCAAs as sole carbon sources [Figure 5].

Other important changes undergone by MABSC exposed to the nutritional environment of the CF airway concerned their surface GPLs. The analysis of the GPL content of SCFM2- and CF sputum-grown MABSC compared to 7H9-ADC-Tween 80-grown bacilli indeed pointed to two significant alterations in the GPL composition of the CF media-grown cells: First was a sharp increase in the production of an as yet unknown form of diglycosylated GPL in which the branched-chain amino alcohol, leucinol, replaced the canonical alaninol at the C-terminus of the peptidyl moiety. Second was an increase in the ratio of triglycosylated to diglycosylated GPLs. The leucinol form of GPL represented >20% of GPLs in SCFM2-grown *Mmas* 604 and 1239 cells and ~ 10% of total GPLs in CF sputum-grown *Mmas* 1239 [Figure 3B]. Interestingly, its production was significantly more pronounced in *Mmas* cells deficient in BCKADH activity suggestive of the increased incorporation of leucine/leucinol into GPLs when the cells cannot efficiently metabolize leucine as a carbon source. Of particular interest was also the observation that the accumulation of both the triglycosylated and leucinol-containing forms of GPLs is strongly stimulated by the presence of mucin in the culture medium [Figure 3]. This finding points to host mucin being an important modulator of the cell surface properties of MABSC in the course of infection and is reminiscent of the recent observation that mucin-associated glycans control the surface properties and the secretion of a broad array of virulence factors in another prominent pathogen of the CF lung, *P. aeruginosa*²⁸.

The fact that these changes in GPL composition of all SCFM2-grown isolates did not reflect in the transcript levels of the gene responsible for the addition of the second rhamnosyl residue (*gtf3*; *MAB_4112c*) or those responsible for the synthesis of the peptidic moiety of GPLs (*mps1* and *mps2*)²⁹ indicates that these changes in the cell surface properties of MABSC under CF growth conditions are independent of transcriptional regulation. In the case of the leucinol moiety, it is possible that the same Mps2 enzyme catalyzes the incorporation of alaninol, valinol and leucinol in GPL, with its activity towards producing leucinol- vs valinol- or alaninol-containing forms of these glycolipids being solely dictated by amino acid availability in the culture medium.

The biological significance of these alterations in the surface GPLs of the bacterium is currently unknown. The comparable growth rate of a WT and GPL-deficient *Mmas* mutant in SCFM2 [Figure S6B] does not support a predominant role for leucinol-containing GPLs in alleviating the potential stress caused by the intracellular accumulation of branched-chain amino keto acids when MABSC switches to BCAAs as major carbon sources during infection. Given the abundance of GPLs at the cell surface, it is possible however that BCAA-derived GPLs alter the interactions of MABSC with host cells, although not reflected in the THP-1 and A549 infection models used in this study. Alternatively or in addition, leucinol-containing GPLs could serve as a leucine storage since leucine appears to be one of MABSC's preferred amino acid-derived carbon sources [Figure 5B]. Besides increasing the polarity of the cell surface, the physiological significance of an increased tri- to di-glycosylated GPL ratio is also not clearly understood. The comparable uptake and replication rates of MABSC grown in SCFM2 with or without mucin in THP-1 and A549 cells excludes a major role for tri-glycosylated GPLs in cell invasion and intracellular persistence.

Cell infection studies indicated that SCFM2-grown bacteria seem to be less prepared to intracellular growth, particularly inside macrophages, compared to those grown in 7H9-ADC-Tween-80. We tentatively attribute this result to the fact that MABSC bacilli located in airway sputum are expected to mainly reside extracellularly, whether growing planktonically or within biofilms.

Another unexpected finding of our study was the absence of significant differences in the drug susceptibility profiles of MABSC isolates planktonically-grown in cation-adjusted Mueller Hinton II broth and in SCFM2 with or without mucin despite noticeable differences in their outer membrane composition. This result indicates that antibiotic susceptibility testing in SCFM2, despite being a closer mimic of the conditions encountered in CF sputum, is unlikely to be more predictive of clinical outcome than the current recommended CLSI protocol. The situation could be different, however, under biofilm-forming conditions where antibiotic tolerance is expected to vary with the nature of the biofilms formed in the different growth media³¹.

Collectively, the studies reported herein yield significant new knowledge about the cell envelope composition and physiological changes undergone by MABSC upon adaptation to the nutritional changes imposed by growth in CF airway sputum. This work further lays the groundwork for future studies aimed at studying how MABSC grown in this environment responds to various host factors (e.g., different mucins) and host-relevant stresses (e.g., pH acidification, decrease in oxygen tension, nitrosative stress, influx of neutrophils, antibiotic treatment, etc.). In this regard, it will be interesting to determine whether any specific responses distinguish clustered *versus* non-clustered MABSC isolates that could account for the global expansion and worse clinical outcome associated with the former isolates⁶.

Methods

Bacterial strains and culture conditions - Reference strains *Mabs* ATCC 19977 and *Mmas* CIP 108297 were obtained from the ATCC and CIP collections, respectively. Clinical isolates from CF patients were from the Papworth University Hospital in Cambridge, UK.

Strains were grown in Middlebrook 7H9 (BD Biosciences) supplemented with 0.5% glycerol and 10% albumin-dextrose-catalase (ADC); in SCFM2¹³; in minimal M63 medium supplemented with 1 mM MgSO₄, 0.05% tyloxapol, and 0.2% glucose; in M63 medium supplemented with 1 mM

MgSO₄, 0.05% tyloxapol and 10% or 20% CF sputum; or in minimal medium (50 mM MOPS, 0.085% NaCl, 50 μM FeCl₃, 0.59 μM MnSO₄, 3.5 μM ZnSO₄, 4.5 μM CaCl₂, 20 mM Asn, 1.6 mM MgSO₄, 2.5 mM Na₂HPO₄/KH₂PO₄, 0.05% tyloxapol, pH 7) containing different concentrations of glucose or BCAAs. See Supporting Text S1 for further details about the CF sputum medium preparation.

Lipid, sugar, mycolic acids and fatty acid analyses – Detailed preparation and analytical procedures for lipids (including GPLs), mycolic acids, fatty acids and sugars are provided in the Supporting Text S1.

Generation of *mmpL4b* and *BCKADH* knockout mutants of *Mmas* CIP 108297 – Knock-out mutants were generated by allelic replacement using a recombineering approach as detailed in the Supporting Text S1.

Cell infections - Adenocarcinomic human alveolar basal epithelial A549 cells and acute monocytic leukemia monocyte-derived THP-1 cells were infected with *Mmas* 1239 and *Mmas* 184 isolates grown in different culture media at a multiplicity of infection (MOI) of 10 as described in the Supporting text S1.

RNA extraction, RNA-seq sample preparation and qRT-PCR - RNA extraction with the Direct-zol™ RNA Miniprep kit (Zymo Research), reverse transcription reactions using the Superscript IV First-Strand Synthesis System (Thermo Fisher) and qRT-PCRs using the SYBR Green PCR Master Mix (Sigma-Aldrich) were conducted as per the manufacturers' protocols and analyzed on a CFX96 real-time PCR machine (Biorad). Details of the RNA-seq sample preparation and data analysis are provided in the Supporting Text S1. Libraries were sequenced using single-end or pair-end reads on an Illumina NextSeq instrument using the high-output 75 cycles or mid-output 150 cycles.

Data Availability - The sequencing data described in this publication have been submitted to the NCBI gene expression omnibus (GEO) under BioProject # PRJNA602697.

Supporting Information

Supporting methods, growth curves, MIC determinations against a panel of clinical isolates, cell envelope analyses, and RNA-sequencing analyses; evidence of gene disruption at the *BCKADH* and *mmpL4b* loci of *Mmas* CIP 108297.

This information is available free of charge on the ACS Publications website.

Corresponding Author: Mary Jackson, Mary.Jackson@colostate.edu

Present/Current Author Addresses: Vinicius Calado Nogueira de Moura; NTM Culture, Biorepository and Coordinating Core, National Jewish Health, Denver, CO 80206

Authors Contributions

CJW, JMB, CA, SKA, DV, RAF, JP, DJO, JAN, MM and MJ designed research. CJW, JMB, CA, SKA, IE, BA, EK, VCNM, DV, JB, KPB, VJ, and KCM performed research. CJW, JMB, CA,

SKA, DV, JB, VJ, MS, JP, DJO, RMD, MM and MJ analyzed data. CJW, JMB, SKA, DJO, MM and MJ wrote the main manuscript text.

All authors reviewed the final version of the manuscript.

Note

The authors declare no competing financial interest.

Abbreviations

BCAA, branched-chain amino acid; BCKADH, branched-chain keto acid dehydrogenase; CF, cystic fibrosis; GC-MS, gas chromatography-mass spectrometry; GPL, glycopeptidolipids; LC-MS, liquid chromatography-mass spectrometry; *Mabs*, *Mycobacterium abscessus* subsp. *abscessus*; MABSC, *Mycobacterium abscessus* complex; *Mmas*, *Mycobacterium abscessus* subsp. *massiliense*; SCFM, synthetic cystic fibrosis medium; WTY, wild-type.

Acknowledgments

This work was supported by an award from the Cystic Fibrosis Foundation (to MJ) and a Strategic Research Centre award (SRC 010) from the Cystic Fibrosis Trust (to MJ, RAF, DJO and JP). CA is supported by the European Union's Horizon 2020 research and innovation program under the Marie Skłodowska-Curie grant No 845479. The content is solely the responsibility of the authors and does not necessarily represent the official views of the sponsors. The funders had no role in study design, data collection and interpretation, or the decision to submit the work for publication.

References

1. Floto, R. A., and Haworth, C. S. (2015) The growing threat of nontuberculous mycobacteria in CF. *J Cyst Fibros* **14**, 1-2
2. Park, I. K., and Olivier, K. N. (2015) Nontuberculous mycobacteria in cystic fibrosis and non-cystic fibrosis bronchiectasis. *Semin Respir Crit Care Med* **36**, 217-224
3. Martiniano, S. L., Nick, J. A., and Daley, C. L. (2019) Nontuberculous Mycobacterial Infections in Cystic Fibrosis. *Thorac Surg Clin* **29**, 95-108
4. Davidson, R. M., Hasan, N. A., de Moura, V. C., Duarte, R. S., Jackson, M., and Strong, M. (2013) Phylogenomics of Brazilian epidemic isolates of *Mycobacterium abscessus* subsp. *bolletii* reveals relationships of global outbreak strains. *Infect Genet Evol* **20C**, 292-297
5. Tettelin, H., Davidson, R. M., Agrawal, S., Aitken, M. L., Shallom, S., Hasan, N. A., Strong, M., Nogueira de Moura, V. C., De Groote, M. A., Duarte, R. S., Hine, E., Parankush, S., Su, Q., Daugherty, S. C., Fraser, C. M., Brown-Elliott, B. A., Wallace, R. J., Jr., Holland, S. M., Sampaio, E. P., Olivier, K. N., Jackson, M., and Zelazny, A. M. (2014) High-level Relatedness among *Mycobacterium abscessus* subsp. *massiliense* Strains from Widely Separated Outbreaks. *Emerg. Infect. Dis.* **20**, 364-371
6. Bryant, J. M., Grogono, D. M., Rodriguez-Rincon, D., Everall, I., Brown, K. P., Moreno, P., Verma, D., Hill, E., Drijkoningen, J., Gilligan, P., Esther, C. R., Noone, P. G., Giddings, O., Bell, S. C., Thomson, R., Wainwright, C. E., Coulter, C., Pandey, S., Wood, M. E., Stockwell, R. E., Ramsay, K. A., Sherrard, L. J., Kidd, T. J., Jabbour, N., Johnson, G. R., Knibbs, L. D., Morawska, L., Sly, P. D., Jones, A., Bilton, D., Laurenson, I., Ruddy, M.,

- Bourke, S., Bowler, I. C., Chapman, S. J., Clayton, A., Cullen, M., Dempsey, O., Denton, M., Desai, M., Drew, R. J., Edenborough, F., Evans, J., Folb, J., Daniels, T., Humphrey, H., Isalska, B., Jensen-Fangel, S., Jonsson, B., Jones, A. M., Katzenstein, T. L., Lillebaek, T., MacGregor, G., Mayell, S., Millar, M., Modha, D., Nash, E. F., O'Brien, C., O'Brien, D., Ohri, C., Pao, C. S., Peckham, D., Perrin, F., Perry, A., Pressler, T., Prtak, L., Qvist, T., Robb, A., Rodgers, H., Schaffer, K., Shafi, N., van Ingen, J., Walshaw, M., Watson, D., West, N., Whitehouse, J., Haworth, C. S., Harris, S. R., Ordway, D., Parkhill, J., and Floto, R. A. (2016) Emergence and spread of a human-transmissible multidrug-resistant nontuberculous mycobacterium. *Science* **354**, 751-757
7. Pawlik, A., Garnier, G., Orgeur, M., Tong, P., Lohan, A., Le Chevalier, F., Sapriel, G., Roux, A. L., Conlon, K., Honore, N., Dillies, M. A., Ma, L., Bouchier, C., Coppee, J. Y., Gaillard, J. L., Gordon, S. V., Loftus, B., Brosch, R., and Herrmann, J. L. (2013) Identification and characterization of the genetic changes responsible for the characteristic smooth-to-rough morphotype alterations of clinically persistent *Mycobacterium abscessus*. *Mol. Microbiol.* **90**, 612-629
 8. Park, I. K., Hsu, A. P., Tettelin, H., Shallom, S. J., Drake, S. K., Ding, L., Wu, U. I., Adamo, N., Prevots, D. R., Olivier, K. N., Holland, S. M., Sampaio, E. P., and Zelazny, A. M. (2015) Clonal Diversification and Changes in Lipid Traits and Colony Morphology in *Mycobacterium abscessus* Clinical Isolates. *J Clin Microbiol* **53**, 3438-3447
 9. Howard, S. T., Rhoades, E., Recht, J., Pang, X., Alsup, A., Kolter, R., Lyons, C. R., and Byrd, T. F. (2006) Spontaneous reversion of *Mycobacterium abscessus* from a smooth to a rough morphotype is associated with reduced expression of glycopeptidolipid and reacquisition of an invasive phenotype. *Microbiology* **152**, 1581-1590
 10. Catherinot, E., Roux, A. L., Macheras, E., Hubert, D., Matmar, M., Dannhoffer, L., Chinet, T., Morand, P., Poyart, C., Heym, B., Rottman, M., Gaillard, J. L., and Herrmann, J. L. (2009) Acute respiratory failure involving an R variant of *Mycobacterium abscessus*. *J Clin Microbiol* **47**, 271-274
 11. Nessar, R., Reyrat, J. M., Davidson, L. B., and Byrd, T. F. (2011) Deletion of the mmpL4b gene in the *Mycobacterium abscessus* glycopeptidolipid biosynthetic pathway results in loss of surface colonization capability, but enhanced ability to replicate in human macrophages and stimulate their innate immune response. *Microbiology* **157**, 1187-1195
 12. Kreutzfeldt, K. M., McAdam, P. R., Claxton, P., Holmes, A., Seagar, A. L., Laurenson, I. F., and Fitzgerald, J. R. (2013) Molecular longitudinal tracking of *Mycobacterium abscessus* spp. during chronic infection of the human lung. *PLoS ONE* **8**, e63237. doi: 10.1371/journal.pone.0063237
 13. Turner, K. H., Wessel, A. K., Palmer, G. C., Murray, J. L., and Whiteley, M. (2015) Essential genome of *Pseudomonas aeruginosa* in cystic fibrosis sputum. *Proc Natl Acad Sci USA* **112**, 4110-4115
 14. Palmer, K. L., Mashburn, L. M., Singh, P. K., and Whiteley, M. (2005) Cystic fibrosis sputum supports growth and cues key aspects of *Pseudomonas aeruginosa* physiology. *J. Bacteriol.* **187**, 5267-5277
 15. Palmer, K. L., Aye, L. M., and Whiteley, M. (2007) Nutritional cues control *Pseudomonas aeruginosa* multicellular behavior in cystic fibrosis sputum. *J. Bacteriol.* **189**, 8079-8087
 16. Jackson, M. (2014) The Mycobacterial Cell Envelope-Lipids. *Cold Spring Harb. Perspect. Med.* **4**, a021105. doi: 10.1101/cshperspect.a021105

17. Etienne, G., Villeneuve, C., Billman-Jacobe, H., Astarie-Dequeker, C., Dupont, M.-A., and Daffé, M. (2002) The impact of the absence of glycopeptidolipids on the ultrastructure, cell surface and cell wall properties, and phagocytosis of *Mycobacterium smegmatis*. *Microbiology* **148**, 3089-3100
18. Viljoen, A., Herrmann, J. L., Onajole, O. K., Stec, J., Kozikowski, A. P., and Kremer, L. (2017) Controlling Extra- and Intramacrophagic Mycobacterium abscessus by Targeting Mycolic Acid Transport. *Front Cell Infect Microbiol* **7**, 388. doi: 10.1111/mmi.13675
19. Caverly, L. J., Caceres, S. M., Fratelli, C., Happoldt, C., Kidwell, K. M., Malcolm, K. C., Nick, J. A., and Nichols, D. P. (2015) Mycobacterium abscessus morphotype comparison in a murine model. *PLoS ONE* **10**, e0117657. doi: 10.1371/journal.pone.0117657
20. Catherinot, E., Clarissou, J., Etienne, G., Ripoll, F., Emile, J.-F., Daffe, M., Perronne, C., Soudais, C., Gaillard, J.-L., and Rottman, M. (2007) Hypervirulence of a rough variant of the *Mycobacterium abscessus* type strain. *Infect. Immun.* **75**, 1055-1058
21. Rhoades, E. R., Archambault, A. S., Greendyke, R., Hsu, F. F., Streeter, C., and Byrd, T. F. (2009) Mycobacterium abscessus Glycopeptidolipids mask underlying cell wall phosphatidyl-myo-inositol mannosides blocking induction of human macrophage TNF-alpha by preventing interaction with TLR2. *J Immunol* **183**, 1997-2007
22. Roux, A. L., Ray, A., Pawlik, A., Medjahed, H., Etienne, G., Rottman, M., Catherinot, E., Coppee, J. Y., Chaoui, K., Monsarrat, B., Toubert, A., Daffe, M., Puzo, G., Gaillard, J. L., Brosch, R., Dulphy, N., Nigou, J., and Herrmann, J. L. (2011) Overexpression of proinflammatory TLR-2-signalling lipoproteins in hypervirulent mycobacterial variants. *Cell. Microbiol.* **13**, 692-704
23. Jonsson, B., Ridell, M., and Wold, A. E. (2013) Phagocytosis and cytokine response to rough and smooth colony variants of Mycobacterium abscessus by human peripheral blood mononuclear cells. *APMIS* **121**, 45-55
24. Bernut, A., Herrmann, J. L., Kissa, K., Dubremetz, J. F., Gaillard, J. L., Lutfalla, G., and Kremer, L. (2014) Mycobacterium abscessus cording prevents phagocytosis and promotes abscess formation. *Proc Natl Acad Sci U S A* **111**, E943-952
25. Roux, A. L., Viljoen, A., Bah, A., Simeone, R., Bernut, A., Laencina, L., Deramaudt, T., Rottman, M., Gaillard, J. L., Majlessi, L., Brosch, R., Girard-Misguich, F., Vergne, I., de Chastellier, C., Kremer, L., and Herrmann, J. L. (2016) The distinct fate of smooth and rough Mycobacterium abscessus variants inside macrophages. *Open Biol* **6**. doi: 10.1098/rsob.160185
26. Whang, J., Back, Y. W., Lee, K. I., Fujiwara, N., Paik, S., Choi, C. H., Park, J. K., and Kim, H. J. (2017) Mycobacterium abscessus glycopeptidolipids inhibit macrophage apoptosis and bacterial spreading by targeting mitochondrial cyclophilin D. *Cell Death Dis* **8**, e3012. doi: 10.1038/cddis.2017.420
27. Clary, G., Sasindran, S. J., Nesbitt, N., Mason, L., Cole, S., Azad, A., McCoy, K., Schlesinger, L. S., and Hall-Stoodley, L. (2018) Mycobacterium abscessus Smooth and Rough Morphotypes Form Antimicrobial-Tolerant Biofilm Phenotypes but Are Killed by Acetic Acid. *Antimicrob Agents Chemother* **62**. doi: 10.1128/AAC.01782-17
28. Wheeler, K. M., Carcamo-Oyarce, G., Turner, B. S., Dellos-Nolan, S., Co, J. Y., Lehoux, S., Cummings, R. D., Wozniak, D. J., and Ribbeck, K. (2019) Mucin glycans attenuate the virulence of *Pseudomonas aeruginosa* in infection. *Nat Microbiol* **4**, 2146-2154
29. Ripoll, F., Deshayes, C., Pasek, S., Laval, F., Beretti, J. L., Biet, F., Risler, J. L., Daffe, M., Etienne, G., Gaillard, J. L., and Reyrat, J. M. (2007) Genomics of glycopeptidolipid

- biosynthesis in *Mycobacterium abscessus* and *M. chelonae*. *BMC Genomics* **8**, 114. doi: 10.1186/1471-2164-8-114
30. Miranda-CasoLuengo, A. A., Staunton, P. M., Dinan, A. M., Lohan, A. J., and Loftus, B. J. (2016) Functional characterization of the *Mycobacterium abscessus* genome coupled with condition specific transcriptomics reveals conserved molecular strategies for host adaptation and persistence. *BMC Genomics* **17**, 553. doi: 10.1186/s12864-016-2868-y
 31. Hunt-Serracin, A. C., Parks, B. J., Boll, J., and Boutte, C. C. (2019) *Mycobacterium abscessus* Cells Have Altered Antibiotic Tolerance and Surface Glycolipids in Artificial Cystic Fibrosis Sputum Medium. *Antimicrob Agents Chemother* **63**. doi: 10.1128/AAC.02488-18

For Table of Contents Use only

